

# Cyanidin 3-*O*- $\beta$ -Galactoside Alleviated Cognitive Impairment in Mice by Regulating Brain Energy Metabolism During Aging

Zhuoyan Fan, Haichao Wen, Xiaoxu Zhang, Jingming Li,\* and Jiachen Zang\*



Cite This: <https://doi.org/10.1021/acs.jafc.1c06240>



Read Online

ACCESS |



Metrics & More



Article Recommendations



Supporting Information

**ABSTRACT:** Metabolic disorder, which commonly happens among senile people worldwide, is an important sign of aging. The early symptoms of neurodegenerative diseases include a decrease in energy metabolism and mitochondrial dysfunction. Comparably, early dietary intervention may be more effective in preventing or delaying brain aging, owing to its role in regulating metabolism. Polyphenol intake has shown its potential in preventing Alzheimer's disease. However, whether there are close connections between polyphenols and the energy metabolism of the brain during aging remains unclear. This study sought to evaluate whether cyanidin 3-*O*- $\beta$ -galactoside from black chokeberry (*Aronia melanocarpa* (Michx.) Elliott) has positive effects on energy metabolism, as well as cognitive function in aging mice. Intragastrical administration of cyanidin 3-*O*- $\beta$ -galactoside (25 and 50 mg/kg/day) for 8 weeks effectively alleviated the decline in brain glucose uptake (decline rate 18.29% versus 1.05%, 7.63%) of aging mice. Moreover, cyanidin 3-*O*- $\beta$ -galactoside also alleviated neuronal damage in the hippocampus (number of neurons  $212.33 \pm 16.19$  versus  $285.33 \pm 29.53$ ,  $301.67 \pm 10.07$ ;  $p < 0.05$ ) and cortex (number of neurons  $82.00 \pm 4.58$  versus  $111.67 \pm 6.51$ ,  $112.00 \pm 1.00$ ;  $p < 0.05$ ). Furthermore, cyanidin 3-*O*- $\beta$ -galactoside reduced  $\beta$ -amyloid load in the brain and significantly increased the crossing-platform number ( $0.92 \pm 1.11$  versus  $1.83 \pm 0.68$ ,  $2.08 \pm 0.58$ ;  $p < 0.05$ ) in the Morris water maze test. We further determined that protein kinase B (AKT) might be the target of cyanidin 3-*O*- $\beta$ -galactoside, which played a beneficial role in controlling the energy metabolism of the brain. These results suggested that early intervention of anthocyanins could promote neuroprotection under the challenge of brain energy metabolism.

**KEYWORDS:** cyanidin 3-*O*- $\beta$ -galactoside, aging, Alzheimer's disease, energy metabolism, cognitive impairment

## INTRODUCTION

Alzheimer's disease (AD) is the most common senile neurodegenerative disease in the world, which is a major threat to the health of the elderly. In the past decade, although great efforts and resources have been devoted to the therapy for AD, most of the drug candidates were often found to have unsatisfactory effects or finally failed to pass clinical trials.<sup>1,2</sup> Aduhelm, a new anti-amyloid drug approved by the US Food and Drug Administration (FDA), is expensive and its clinical benefits need to be further verified.<sup>3</sup> In addition, the efficacy of  $\beta$ -amyloid ( $A\beta$ )-based therapeutic strategies will depend on whether it can prevent the further progress of AD pathology, such as how many neurons in the brain region have already been irreversibly damaged. Once amyloid triggers an irreversible cascade reaction, the disease continues to develop even after removing amyloid deposits.<sup>4</sup> At present, the four mainstream drugs used for AD, rivastigmine, galantamine, donepezil, and memantine, can improve symptoms but cannot effectively prevent the onset or reverse the course of the disease, which may even produce adverse reactions.<sup>5</sup> Furthermore, the cost of treatment of AD is expected to be \$1 trillion by 2030,<sup>6</sup> which may lead to a severe burden for the patients' families. Thus, the prevention and treatment of AD have become a global challenge.

The abnormal energy metabolism is an important manifestation of aging.<sup>7</sup> The decreased consumption of glucose occurs among not only the elderly but also dementia patients

because glucose is the main fuel for the brain.<sup>8,9</sup> The energy metabolism of the brain decreases with aging, which usually occurs before the clinical manifestations and pathological features of neurodegenerative diseases, such as neuronal apoptosis, loss of neuronal and synaptic connections, and mitochondrial dysfunction.<sup>10</sup> Thus, the impairment of brain energy metabolism may play a key role in the pathology of neurodegenerative diseases. In another word, it may be the initiating factor of neurodegenerative diseases, especially for the occurrence and aggravation of AD.<sup>11,12</sup> In recent years, cerebral glucose metabolism has been a reliable biomarker for the diagnosis of many neurodegenerative diseases.<sup>13</sup>

Except for clinic treatment, dietary prevention has also been an alternative strategy for AD intervention. In recent years, plant-derived polyphenols are of great favor because of their immense therapeutic potential for AD. For example, flavanols derived from lychee seed significantly inhibited Tau hyperphosphorylation and improved the cognitive function of rats.<sup>14</sup> Phenolic acids inhibited acetylcholinesterase (AChE) and butyrylcholinesterase (BChE) and inhibited the formation of

**Received:** October 5, 2021

**Revised:** December 28, 2021

**Accepted:** January 1, 2022

$A\beta$  fibrils.<sup>15</sup> The benefits of stilbenes for cognitive function and neuroprotection have also attracted widespread attention.<sup>16</sup> The significant antioxidant and anti-inflammatory activities of anthocyanins have been widely reported and confirmed. Most noteworthy, anthocyanins can improve AD by protecting neurons and glial cells from the damage of  $A\beta$  fibrils, glutamate, and lipopolysaccharide.<sup>17</sup> According to the previous report, both in vivo and in vitro evidence support the fact that dietary anthocyanins are able to penetrate the blood–brain barrier (BBB) and enter the brain tissue, where they perform neuroprotective activity and improve cognitive function to prevent neurodegenerative diseases.<sup>17,18</sup> Anthocyanins stayed in nerve tissue for a period of time, which may increase their direct effect on brain function.<sup>18,19</sup> Moreover, an in vitro study showed that anthocyanins accumulated in brain endothelial cells and cross the BBB cell model in a time-dependent manner within 1 h.<sup>20,21</sup> Many studies have focused on the role of anthocyanins in protecting neurons from damages and apoptosis by  $A\beta$ , glutamate, and lipopolysaccharide, as well as reducing oxidative stress to enhance cognitive and memory functions.<sup>17</sup> However, the relationships between anthocyanins and early metabolism of AD remain unknown, which may be conducive for clarifying the potential of anthocyanins as a nutritional intervention for AD and other neurodegenerative diseases.

Cyanidin 3-*O*- $\beta$ -galactoside (Cy3Gal) is a kind of anthocyanin that was purified from black chokeberry (*Aronia melanocarpa* (Michx.) Elliott) in our previous study.<sup>22</sup> Compared with other aglycons, the galactoside-bound anthocyanins can be absorbed faster in the body.<sup>23</sup> In addition, we found that Cy3Gal has a strong antioxidant capacity and neuroprotective effects, which improves learning and memory impairment in  $A\beta$ -induced rats.<sup>22</sup> To uncover the possible mechanism, we hypothesized that Cy3Gal could regulate brain energy metabolism and further improve cognitive impairment. In this study, we investigated the effects of Cy3Gal on the brain energy metabolism, the clinical manifestations, and pathological characteristics of late-onset AD in senescence-accelerated mouse-prone 8 (SAMP8) model mice. We found that Cy3Gal likely targeted AKT and played a beneficial role in the regulation of brain energy metabolism, which significantly alleviated AD symptoms in aging mice. Our results suggested that an early dietary supplement of Cy3Gal may help improve brain energy metabolism during aging, potentially reducing the incidence of AD.

## MATERIALS AND METHODS

**Chemicals.** Cy3Gal with 95% purity from black chokeberry (*A. melanocarpa* (Michx.) Elliott) was provided by Anhui HaoChen Ecological Agriculture Development Co., Ltd. (Anhui, China). <sup>18</sup>F-Fluorodeoxyglucose (<sup>18</sup>F-FDG) radiotracer and <sup>18</sup>F-florbetapir (<sup>18</sup>F-AV45) radiotracer were purchased from Anhui Ma'anshan Biotechnology Co., Ltd. (Anhui, China). Bax, Bcl-2, cleaved caspase-3, cleaved caspase-9, and horseradish peroxidase binding secondary antibodies were purchased from Cell Signaling Technology (Danvers, MA).  $A\beta_{1-42}$  and HRP goat antirabbit IgG secondary antibodies were purchased from Abcam Company (Cambridge, U.K.). The BCA protein concentration assay kit was purchased from Shanghai BiYunTian Biotechnology Co., Ltd. (Shanghai, China). The DAB kit was purchased from Dako Denmark A/S (Glostrup, Denmark). The HE staining kit was purchased from Beyotime (Beijing, China). All other chemicals were of analytical grade.

**Experimental Animals.** Four-month-old male SAMP8 and senescence-accelerated mouse-resistant (SAMR1) mice (weighing

$20 \pm 2$  g) were purchased by Animal Resources Center in First Teaching Hospital of Tianjin University of Traditional Chinese Medicine (Tianjin, China). All mice were kept in a temperature-controlled ( $22 \pm 2$  °C) animal facility under a 12 h dark–light cycle. Water and food were available ad libitum. After 1 week of adaption, SAMP8 mice were randomly divided into three groups ( $n = 10$  each group) as follows: SAMP8, in which mice were orally administered with 0.2 mL of sterile water as the model group; Cy3Gal-High, in which mice were orally administered with a high dose of Cy3Gal dissolved in 0.2 mL of sterile water (50 mg/kg/day b.w.); and Cy3Gal-Low, in which mice were orally administered with a low dose of Cy3Gal dissolved in 0.2 mL of sterile water (25 mg/kg/day b.w.). The SAMR1 group, in which the mice were orally administered with 0.2 mL of sterile water, was the control group.

Radiation imaging was performed before and after the administration. All mice were subjected to behavioral tests after 8 weeks of administration and anesthetized 2 weeks after the last behavioral test. All experiments were approved by the Animal Ethical and Welfare Committee (No. NKYYDWLL-2019-105).

**Rotarod Test.** The rotarod test was performed as previously described.<sup>24,25</sup> The diameter and length of the rotating rod were 30 and 60 mm, respectively. The speed range of the rotating rod was 5–40 rpm. Before the test, the mice were placed on a rotating stick for 3 min to adapt and were trained for 1 min. In the test, the speed of the rotating rod was accelerated from 4 to 40 rpm for 180 s. The test was repeated four times and the latency to fall was recorded.

**Radiological Imaging.** Mice were fixed with a fixator and injected with about 200  $\mu$ Ci of <sup>18</sup>F-fluorodeoxyglucose (<sup>18</sup>F-FDG) radiotracer through the tail vein after 6 h fasting. The initial dose, measurement time, injection time, residual amount of syringe after injection, and detection time were recorded accurately. After the injection, the mice were placed in the anesthesia box and given isoflurane gas at a flow rate of 3 L/min for 5–10 min. The mice were fixed and placed in micro-positron emission tomography/computed tomography (PET/CT) with an Inveon multimodality micro-PET/SPECT/CT scanner (Siemens Medical Solutions). The dynamic PET monitoring and CT scanning were performed on the mice. During the scanning, isoflurane gas was continuously injected. The uptake value of radioactive substances in the brain was recorded, and the standard uptake value (SUV) was analyzed by the Inveon Research Workplace software (Siemens). The PET/CT images were processed using the PMOD software (version 3.4, PMOD Technologies Ltd., Zurich, Switzerland).

The monitoring method of  $A\beta$  is similar to that of glucose. In short, about 100  $\mu$ Ci of <sup>18</sup>F-florbetapir (<sup>18</sup>F-AV45) was injected into mice via tail vein and then scanned by PET/CT.

**Nissl Staining.** Nissl staining of brain tissue was performed as previously described.<sup>25</sup> The mice were euthanized and perfused with normal saline. Then, the brains were found and put in 4% paraformaldehyde. Serial coronal sections with a thickness of 25  $\mu$ m were cut using a cryostat (Leica Microsystems, Wetzlar, Germany). The sections were washed twice for 5 min in 0.01 M PBS and incubated in 1% toluidine blue staining solution for 5–10 min at 20–25 °C. Then, the sections were rinsed in distilled water, soaked in 95% ethanol for 30 min, and dehydrated in 100% ethanol. After dehydration, the sections were placed in xylene and cover-slipped using a resin medium. The neurons in the hippocampus and cerebral cortex were quantified using Image J-Pro Plus software (developed by Wayne Rasband from NIH).

**Western Blot.** The brains of the mice were immediately placed in liquid nitrogen. The frozen brains were homogenized in protein lysate buffer and centrifuged at 4 °C for 15 min at 12 000g. A Bio-Rad protein assay (Beyotime, Beijing, China) was used to determine protein concentrations. The protein samples were separated by SDS-PAGE, transferred to the poly(vinylidene fluoride) (PVDF) membrane, and sealed with 5% skim milk for 2 h. The PVDF membrane was then incubated with a specific primary antibody at 4 °C. Horseradish peroxidase binding secondary antibodies were incubated with the PVDF membrane. The proteins were visualized

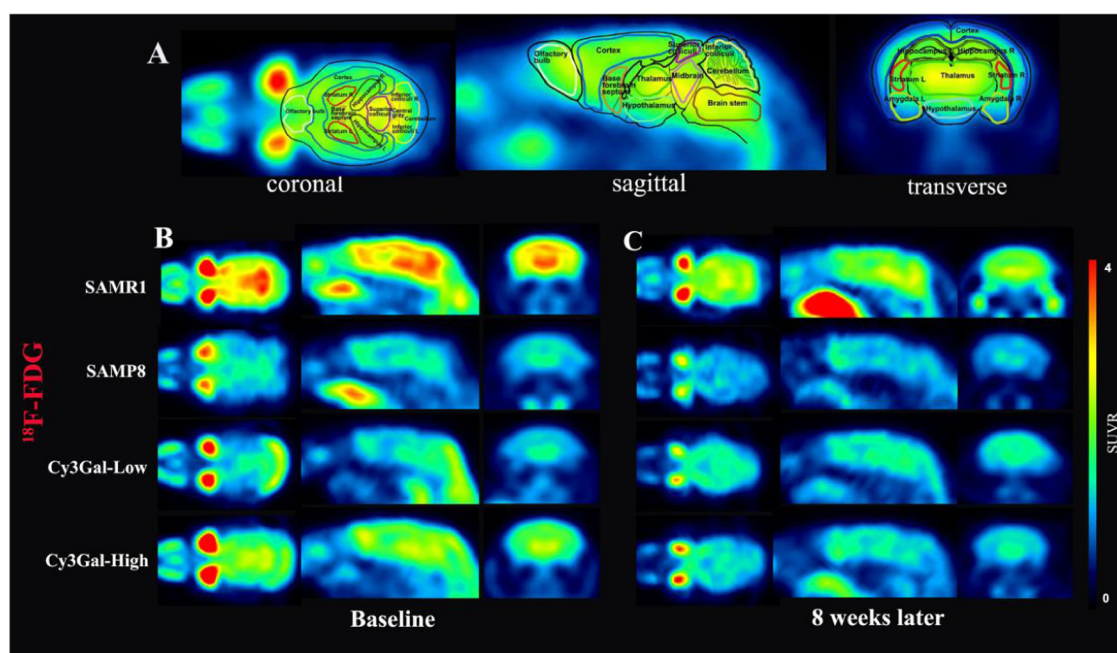


**Figure 1.** Cy3Gal improved glucose uptake in the brain of aged mice ( $n = 8$ ). (A) Images of different regions in a mouse brain visualized by the PET scan of  $^{18}\text{F}$ -FDG (upper panels). Representative radiology images of the glucose metabolism in mice brains of different groups before (B) and after 8 weeks of (C) administration with Cy3Gal.  $^{18}\text{F}$ -FDG uptake in the mice brains of different groups was assessed by measuring the standard uptake value ratio (SUVR), and the higher ratio the more  $^{18}\text{F}$ -FDG uptake.

by chemiluminescence reagents and analyzed by the gel recording system (GelDoc It 310 imaging system).

**Morris Water Maze Test.** After 8 weeks of intragastric administration with Cy3Gal, the Morris water maze (MWM) test was performed as previously described.<sup>25</sup> The circular pool was 120 cm in diameter and 40 cm in depth with an invisible platform (Beijing Zhongshidichuang Technology Development Co., Ltd. Beijing, China). The water in the pool was mixed with black ink. During the experiment, the temperature of the water remained at 22–24 °C, and all landmarks around the maze remained the same. The MWM test included spatial learning and acquisition trials (hidden platform trials) and a spatial probe trial. Before the spatial acquisition trials, each mouse was put into the water to adapt for 2 min, and the platform, located in the middle of the first quadrant for 1 day, was visible. Then, water was added to the pool with the platform 1 cm below the water surface. During the hidden platform trials, each mouse was placed into the water from one of the start positions, facing the wall. The spatial acquisition trials were conducted over 5 days with four trials per day. If an animal reached the platform, the timer was stopped. If an animal failed to find the platform within 90 s, it was placed on the platform for 15 s to learn the platform's location. The spatial probe test was conducted on day 7, and the platform was removed. Then, the mice were put into the water from the opposite quadrant of the quadrant with the platform. The swimming route, the time in the target quadrant, and the times of crossing the platform by the mice were recorded. After testing, the mice were dried with a towel to keep them warm. The test was recorded with a video camera, and the data were analyzed using ANY-maze behavioral tracking software (Stoelting Co., Wood Dale, IL).

**Nesting Behavior.** The nesting test was performed as previously described by Deacon et al.<sup>26</sup> Briefly, new wood shavings were put into the mouse cage to make the bottom flat with 32 pieces of soft paper (4.5 cm  $\times$  4.5 cm) were laid on. After 24 h, the ability of mice to nest was evaluated, and scores were given.

**Immunohistochemical and Hematoxylin–Eosin Staining.** Mice were euthanized and perfused with normal saline. Then, the brains were found and put in 4% neutral paraformaldehyde for 24 h. Paraffin sections were dewaxed with xylene and dehydrated with different gradients of ethanol until differentiation. A total of 0.01 mol/

L citric acid buffer was put into slices and heated in a microwave oven for antigen repair. Goat serum blocking solution was used for 20 min. An  $\text{A}\beta_{1-42}$  antibody diluent (1:100) was added and incubated overnight at 4 °C. An HRP goat antirabbit IgG secondary antibody (1:2000) was added and incubated at 37 °C for 30 min. A streptavidin peroxidase conjugate was added and incubated at 37 °C for 30 min. A DAB kit was added for 5–20 min. The nuclei were slightly stained with hematoxylin. The sections were scanned, and the deposition of amyloid proteins was observed to be brown under the microscope. Image J-Pro Plus software (developed by Wayne Rasband from NIH) was used for the statistical analysis. For histological examination, brain tissues were embedded in paraffin for staining with hematoxylin and eosin (HE).

**Molecular Dynamics Simulation.** The structures of Akt protein (PDB ID: 4GV1) and PI3K protein (PDB ID: 3HHM) were from the PDB database. The structure of Cy3Gal was from PubChem (CID: 441699). Autodock Vina was used for molecular docking of protein and Cy3Gal complex conformation (<http://autodock.scripps.edu>). The molecular properties of the box were calculated and simulated using Chemistry at HARvard Macromolecular Mechanics 36 (CHARMM 36). PyMOL was used for drawing (<http://www.pymol.org/>). The hydrogen bond and hydrophobic interaction were analyzed by ligplot<sup>+</sup>.

**Statistical Analysis.** SUVmean was automatically extracted from all regions of interest (ROIs) and then used to calculate SUVR using the cerebellum as the reference region ( $\text{SUVR} = \text{SUVmean}/\text{cerebellum SUVmean}$ ).

Data are presented as mean  $\pm$  standard deviation. The test data were processed by one-way ANOVA using the SPSS version 20.0 software package. Multiple comparisons of the data were performed via Tukey's test, which was used to compute significant differences at  $p < 0.05$  and  $p < 0.01$ .

## RESULTS

**Cy3Gal Improved Energy Metabolism in the Brain of Aged Mice.** To investigate the effects of Cy3Gal in brain energy metabolism, the forced exercise endurance of aged mice was tested by a rotating bar to analyze their energy

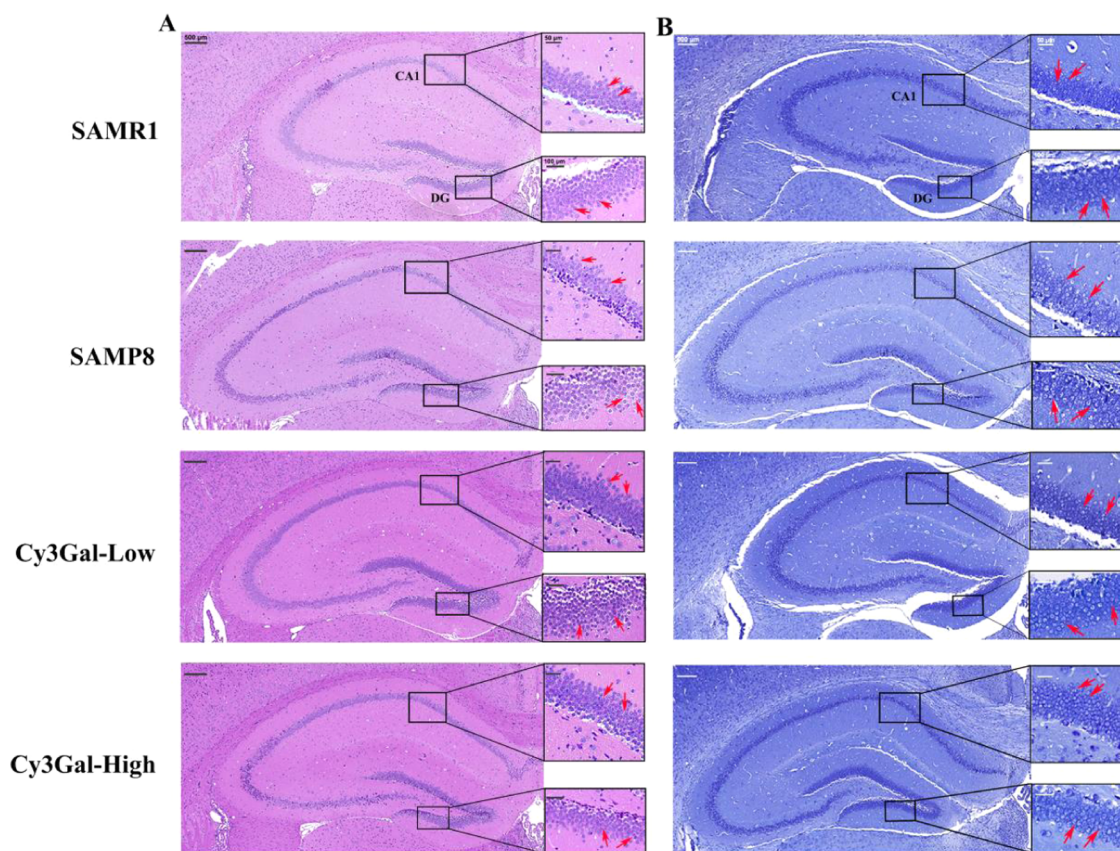


**Figure 2.** Histological examinations of the hippocampus region in mice brains ( $n = 6$ ). Representative images of HE staining (A) and Nissl staining (B) of the hippocampus region in mice from different groups. Hippocampus CA1 (the rectangle at top right) and dentate gyrus (DG, the rectangle at bottom right) regions were examined. The red arrows indicated neurons.

expenditure. Compared with that of the SAMR1 mice, the movement ability of the SAMP8 mice decreased significantly. After the 8-week intervention, the treatment with Cy3Gal-High led to a significant effect on improvement in exercise endurance, rather than the treatment with Cy3Gal-Low. Collectively, Cy3Gal improved energy metabolism and promoted the movement ability of aged mice (Supplementary Figure 1).

ATP, 95% or more of which is produced by glucose metabolism, is the main currency of brain energy metabolism.<sup>27</sup> In view of the beneficial effects of Cy3Gal as shown above, we dynamically monitored the glucose metabolism in the brain of aged mice. The PET/CT technology is commonly used to identify and localize metastases of malignant diseases. The application of PET/CT can sensitively, accurately, and specifically provide detailed molecular information, such as the function and metabolism of the lesion.<sup>28</sup> We examined the effects of Cy3Gal on glucose metabolism in different regions of the mouse brain by PET/CT and quantified glucose metabolism by the standard uptake value ratio (SUVR) of the <sup>18</sup>F-FDG (Figure 1A). Eight weeks later, the SUVR had no significant difference in SAMR1 mice (Supplementary Figures 2 and 3) but was decreased obviously in almost all of the brain regions of SAMP8 mice, implying that the glucose metabolism significantly decreased with aging (Figure 1B,C and Supplementary Figures 2 and 3). In comparison, the <sup>18</sup>F-FDG uptake in the brain of the Cy3Gal-Low group mice was not decreased, especially in the hippocampus, cerebral cortex, olfactory bulb, striatum, superior colliculus, inferior colliculus, midbrain,

cerebellum, thalamus, central gray matter, and brain stem regions (Supplementary Figures 2 and 3). For mice treated with a high dose of Cy3Gal, no significant increase was found in total glucose uptake of the brain (Supplementary Figure 3). The low <sup>18</sup>F-FDG uptake in the olfactory bulb, midbrain, and central gray matter regions might result in the phenomenon (Supplementary Figure 2). This might result in the phenomenon of no significant improvement in total brain glucose intake in mice treated with a high dose of Cy3Gal (Supplementary Figure 3). All in all, there was a positive correlation between Cy3Gal intervention and brain glucose uptake (Supplementary Figure 4). The 8-week intervention of Cy3Gal had a beneficial effect on the energy metabolism in mice brains during aging.

**Cy3Gal Alleviated Neuronal Damage of Aged Mice.** It is commonly known that neurodegenerative diseases, such as AD, are directly related to neuronal damage in the hippocampus and cerebral cortex.<sup>29</sup> Thus, we further explored if Cy3Gal had protective effects on neurons in aged mice. As shown in Figure 2, the result of HE staining demonstrated that the neurons in the hippocampus of SAMR1 mice were arranged tightly and orderly with clear nuclei, as indicated by red arrows in Figure 2A. However, in the SAMP8 mice, the neurons adopted a more disorderly arrangement, and the chromatin of the neuron nucleus was dense and condensed, displaying nuclear pyknosis (as indicated by red arrows), accompanied by apoptosis and loss of a large number of neurons (Figure 2A and Supplementary Figure 5). After the administration of Cy3Gal to the SAMP8 mice, the neurons in

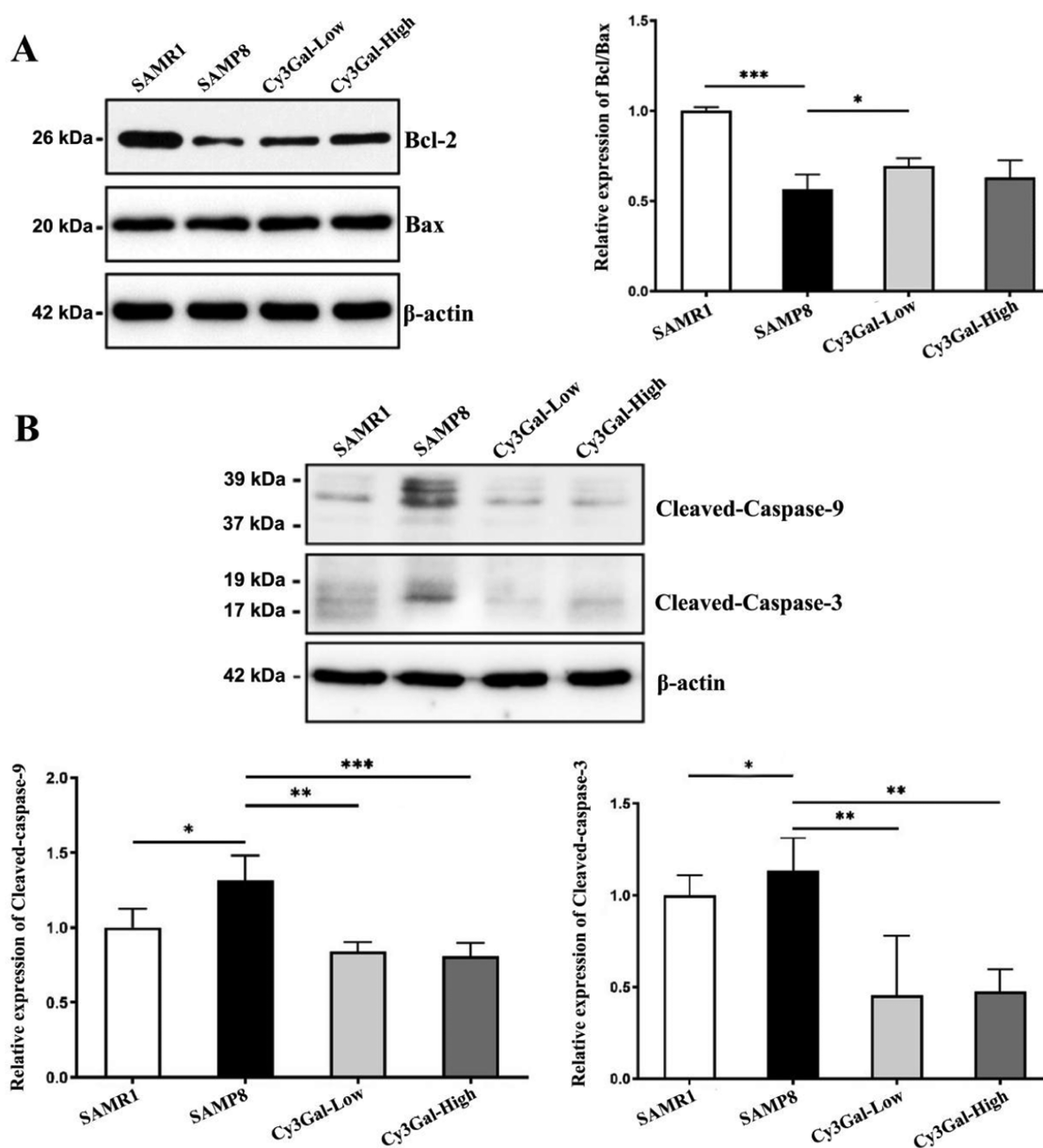


**Figure 3.** Effects of Cy3Gal on mitochondrial function and neuron apoptosis in aged mice ( $n = 4$ ). Representative Western blot images and analysis of Bcl-2 and Bax (A), cleaved caspase-9, and cleaved caspase-3 (B). \* $p < 0.05$ , \*\* $p < 0.01$ , and \*\*\* $p < 0.001$ .

the hippocampi were round (or oval) and tightly arranged with light blue nuclei, as observed in CA1 and DG regions in Figure 2A (as indicated by red arrows). Cy3Gal improved the remarkable reduction in neuronal loss in the hippocampus of the SAMP8 mice (Supplementary Figure 5). The results of Nissl staining were similar to those of HE staining. Neurons exhibited a normal morphology with distinct round or oval nuclei and nucleoli, and clear Nissl bodies in the cytoplasm in the SAMR1 mice. In comparison, a large number of atrophic neurons with damaged nuclei and shrunken cytoplasm were observed in the SAMP8 mice, and most neurons showed a loss of Nissl bodies (as indicated by red arrows). Cy3Gal improved the morphology of neurons (like what was displayed in CA1 and DG regions), as well as markedly reversed age-induced neuronal loss, although the effects did not depend on the dose (Figure 2B and Supplementary Figure 5). By HE and Nissl staining, the improvement of Cy3Gal on neuronal degeneration with loss was also observed in the cerebral cortex of the

SAMP8 mice (Supplementary Figures 6 and 7). Those results suggested that Cy3Gal had a potential neuroprotective effect by alleviating the damage and apoptosis of neurons in aged mice.

**Cy3Gal Regulated the Key Regulators of Mitochondrial Function and Neuron Apoptosis.** Mitochondria is the powerhouse supplying energy for life and its structures and functions are closely related to energy metabolism. At the same time, mitochondria are also the central regulators of apoptosis in vertebrates. In view of the beneficial effects of Cy3Gal on energy metabolism and neurons, we first examined mitochondrial membrane proteins, B-cell lymphoma-2 (Bcl-2) and Bcl-2-associated X (Bax). Compared with that of the SAMR1 mice, the expression ratio of Bcl-2 and Bax decreased remarkably in the brain of the SAMP8 mice. After the administration with low dose of Cy3Gal for 8 weeks, the expression ratio of Bcl-2 and Bax in the SAMP8 mice was upregulated, but no significant effect was observed in the mice treated with high

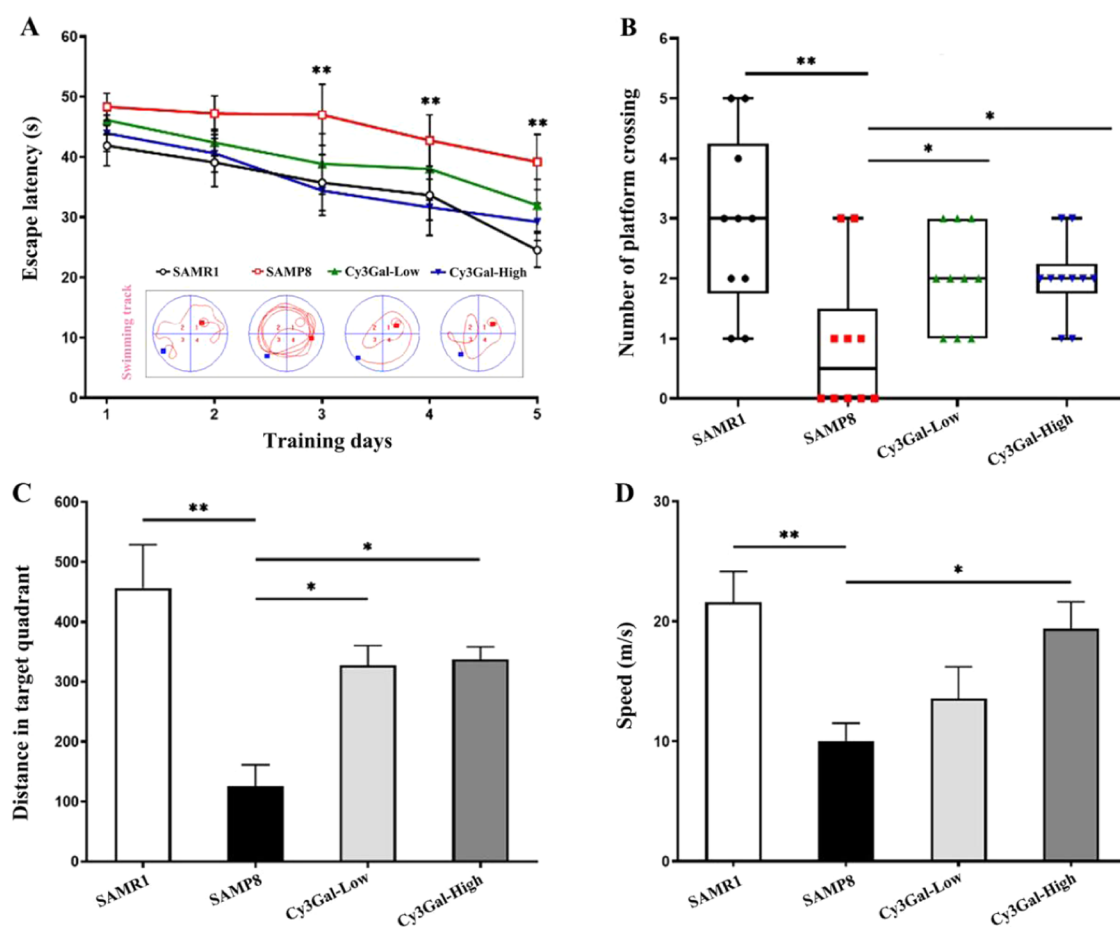


**Figure 4.** Effects of Cy3Gal on spatial learning and memory abilities of aged mice ( $n = 6$ ). The escape latency time of mice looking for a safe platform in the spatial acquisition trials over 5 days. Inset in (A) shows representative action tracks of mice of different groups in the Morris water maze test (A). Times mice crossed the platform in the spatial probe test (B). Total movement distance in the target quadrant in the spatial probe test (C). Swimming speed (m/s) of mice in the spatial probe test (D). \*\* $p < 0.01$  and \* $p < 0.05$ .

dose of Cy3Gal (Figure 3A). Thus, Cy3Gal improved the mitochondrial membrane permeability in the brain of aged mice to a certain extent.

Caspases are the key enzymes in the mitochondria-dependent apoptosis pathway, in which caspase-9 and caspase-3 are the major effectors in the process of apoptosis.<sup>30</sup> The interaction between antiapoptotic protein Bcl-2 and proapoptotic protein Bax can regulate the permeability of the mitochondrial outer membrane, and thus regulate apoptosis through caspase-9- and caspase-3-dependent pathways.<sup>31</sup> We observed that Cy3Gal significantly inhibited the activation of caspase-9 and caspase-3, while they were obviously activated in the brain of the SAMP8 mice. As shown in Figure 3B, the expressions of the cleaved caspase-9 and cleaved caspase-3 were significantly reduced after administration with Cy3Gal. Overall, Cy3Gal displayed the potential to inhibit neuron apoptosis involving the mitochondrial pathway in aged mice. The results were consistent with the neuroprotective effects as shown in histological examinations (Figure 2 and Supplementary Figure 6).

**Cy3Gal Improved the Cognitive and Memory Abilities of Aged Mice.** To explore whether the improvement in energy metabolism by Cy3Gal helped to delay AD, we performed the MWM test to evaluate the spatial memory and behavioral ability of aged mice. In the spatial acquisition test, the escape latency looking for a safe platform decreased

gradually by training. Obviously, the difference between the SAMP8 mice and the SAMR1 mice increased with the progression of time, as shown in Figure 4A, which may be caused by the metabolic disorder and neural damage. The SAMP8 mice displayed age-related learning abilities relative to the SAMR1 mice. Interestingly, the intake of Cy3Gal narrowed the gap between the SAMR1 mice and the untreated SAMP8 mice. Similar to the results of a spatial acquisition test, Cy3Gal also significantly increased the times of the SAMP8 mice to cross the safe platform (Figure 4B). The results indicated that Cy3Gal had a protective effect on spatial learning and memory impairments in aged mice.

Notably, Cy3Gal increased the total swimming distance and speed of the SAMP8 mice (Figure 4C,D), which was consistent with the improvement of exercise endurance in the rotating rod test (Supplementary Figure 1). Nesting can be used as an indicator of cognitive dysfunction in the pathological process of AD.<sup>32</sup> The nesting test showed that the average score of nesting in the SAMR1 mice was  $3.83 \pm 0.40$  (the total score was 5), and the mice used paper to build a clean bowl-shaped nest with feces concentrated on the other side of the nest. In contrast, SAMP8 mice only scored  $1.83 \pm 0.75$ . The SAMP8 mice could build cup-shaped nests with paper scattered around the nest after the administration of low dose and high dose of Cy3Gal, and the mice scored  $3.00 \pm 0.63$  and  $2.83 \pm 0.98$ , respectively (Supplementary Figure 8).

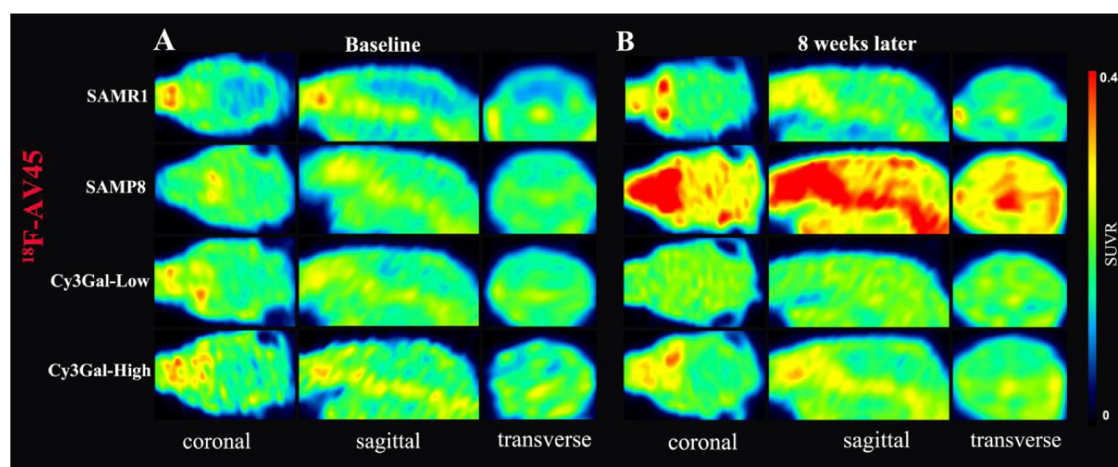


**Figure 5.** Effects of Cy3Gal on the  $A\beta$  accumulation in the brain of aged mice. Representative radiology images of  $^{18}\text{F}$ -AV45 uptake in mice brains of different groups before (A) and after 8-week (B) administration with Cy3Gal.  $^{18}\text{F}$ -AV45 uptake in mice brains of different groups was assessed by measuring the SUVR; the higher ratio, the higher the  $^{18}\text{F}$ -AV45 uptake.

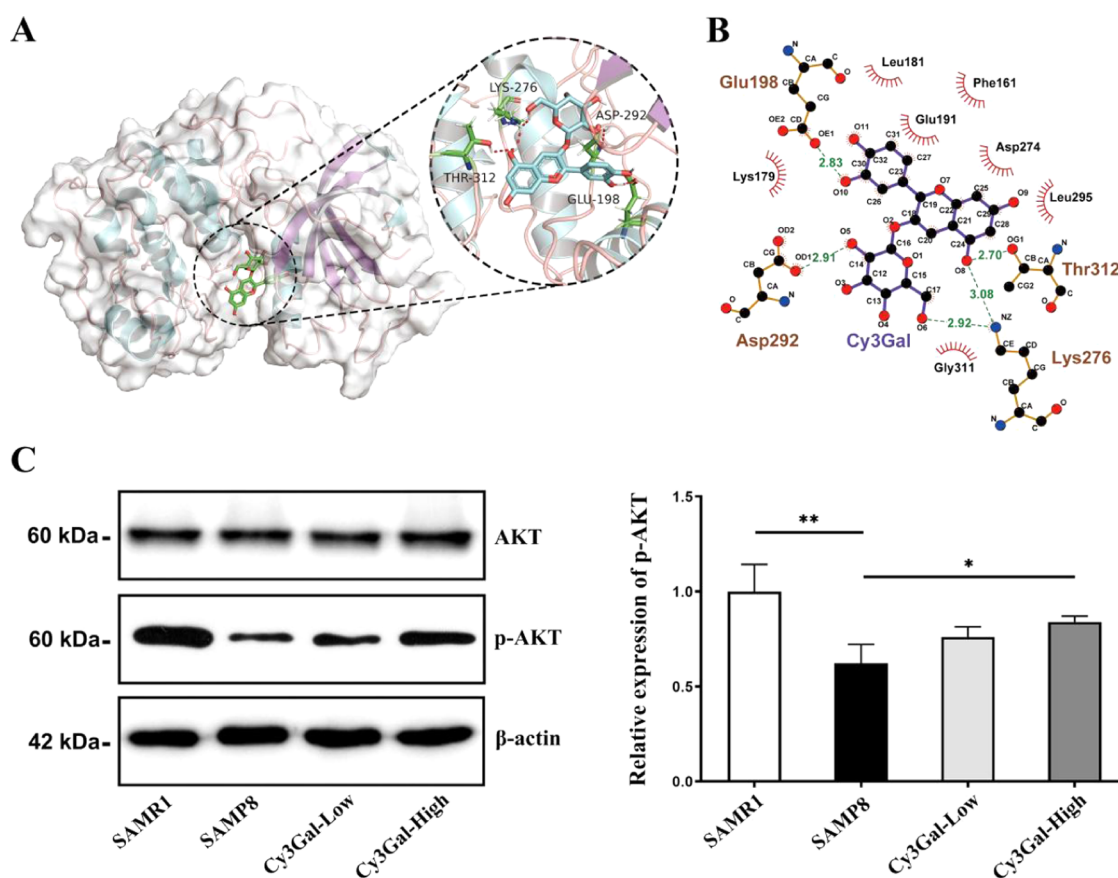


**Figure 6.** Interaction between Cy3Gal and Akt. Molecular docking of the interaction between AKT and Cy3Gal: (A) complex view and (B) binding simulation analyses of 2D interactions between AKT and Cy3Gal. (C) Representative Western blot images and analysis of activated AKT in mice brains ( $n = 4$ ). \* $p < 0.05$  and \*\* $p < 0.01$ .

Those results indicated that Cy3Gal effectively improved the behavioral abilities of aging mice, which has the potential to improve cognitive dysfunction.

**Cy3Gal Reduced  $A\beta$  Accumulation in Brain of Aged Mice.** The abnormal accumulation of  $A\beta$  in the central nervous system was one of the important signs of AD.  $^{18}\text{F}$ -AV45 PET, had high affinity, sensitivity, and specificity with  $A\beta$ , was used to mark the  $A\beta$  load.<sup>33</sup> Through brain imaging

analysis, PET images were visually analyzed to evaluate the distribution of radioactive  $^{18}\text{F}$ -AV45 in each brain region of mice, and the SUVR of  $^{18}\text{F}$ -AV45 was calculated to evaluate the value of  $A\beta$  load. A small amount of  $^{18}\text{F}$ -AV45 was deposited in the brain SAMR1 mice after 8 weeks when  $^{18}\text{F}$ -AV45 deposition increased remarkably in the brain of the SAMP8 mice (Figure 5B). In the SAMP8 mice, the  $A\beta$  load increased in the hippocampus, basal forebrain, olfactory bulb,

striatum, midbrain, superior colliculus, hypothalamus, thalamus, and central gray matter, while  $A\beta$  mainly accumulated in the olfactory bulb region of the SAMR1 mice (Supplementary Figure 9). Low and high doses of Cy3Gal displayed significant improvement effects of the  $A\beta$  load (Figure 5B), as shown in Supplementary Figure 9. Cy3Gal significantly reduced the range and degree of  $A\beta$  load in the brain of the SAMP8 mice. The results were verified by the immunohistochemistry analysis for mice brain tissue in different groups. Large amounts of plaques accumulated in the hippocampus (Supplementary Figure 10A) and cerebral cortex (Supplementary Figure 10B) of the SAMP8 mice, where the levels of plaque decreased after the Cy3Gal administration. The results suggested that early intervention of Cy3Gal delayed the pathological progression related to AD in the mice brains during aging.

**Cy3Gal Likely Targeted Akt Factor.** We next explored the possible effect of Cy3Gal on improved cognitive impairment and energy metabolism in the brain. PI3K/Akt signaling plays an important role in the regulation of energy metabolism and apoptosis. At the same time, the abnormal control of the PI3K/Akt axis is considered to be the pathogenic node of AD, and the abnormal PI3K/Akt signaling is considered to be the early feature of AD.<sup>34</sup> Therefore, it is most probable that Cy3Gal might affect the PI3K/Akt pathway, leading to the beneficial effects on neuroprotection. To verify our hypothesis, we first used molecular dynamics simulation to predict the interactions between Cy3Gal and PI3K/Akt. Molecular docking results showed that the binding of Cy3Gal with PI3K was weak (Supplementary Figure 11A,B and Supplementary Table 2). However, the combination of Cy3Gal and Akt was much stronger, stabilized by both hydrogen bonds and hydrophobic forces. As shown in Figure 6A,B, Cy3Gal was buried in the hydrophobic cavity of Akt, surrounded by five hydrogen bonds (Glu198, Asp292, Thr312, and Lys276) and two hydrophobic interactions (Asp274 and Phe161). Notably, Asp274 and Phe161 are precisely the metabolic sites of Akt. Consistent with the results of molecular docking, Cy3Gal promoted the activation of Akt in the mice brains but not PI3K (Figure 6C and Supplementary Figure 11C). The results suggested that Cy3Gal was bound to the active site of Akt and activated downstream signal pathway.

## DISCUSSION

Early diagnosis of AD is crucial for early and effective therapeutic interventions and reduces the risk of AD. PET can be used to analyze the glucose utilization of the brain, and it is considered to be the most reliable tool for the early diagnosis of AD.<sup>35</sup> In this study, we used PET/CT to monitor the changes in energy metabolism in the mice brains during aging to further evaluate the effects of early intervention on AD-related pathologies and symptoms. Brain glucose metabolism has become an important tool for the diagnosis of many brain diseases, including neurodegenerative diseases.<sup>13</sup> For patients with AD, a decline in glucose utilization in the brain (especially in the hippocampus and cerebral cortex) is related to learning, memory, and cognitive impairment.<sup>36</sup> Moreover, the decrease of brain glucose uptake has been considered an early and accurate biomarker of AD neural atrophy and dysfunction.<sup>37</sup> More and more evidence shows that the disorder of brain energy metabolism occurs in the preclinical stage of AD before pathological changes and eventual cognitive impairment.<sup>38,39</sup> The disorder of energy metabolism in the brain further

promotes the pathological process of AD by inducing oxidative stress and blocking the production of neurotransmitters.<sup>40</sup> On the other hand, the toxic protein, such as  $A\beta$  aggregates, in brains may induce mitochondrial dysfunction and oxidative stress and thus accelerate the disorder of energy metabolism, finally forming a vicious circle.<sup>41</sup> Thus, here we provided a potential strategy for the treatment of AD from the perspective of energy metabolism, and significant effects were observed.

Nearly 95% of AD patients were sporadic AD (sAD) without a family history. sAD is the most prevalent form of age-related dementia.<sup>42</sup> Therefore, the appropriate animal model is also crucial for further elucidating the pathogenesis of sAD and the development of effective drugs. We used SAMP8 as an AD mouse model to investigate the cognitive effects of Cy3Gal administration. The SAMP8 mice have significant advantages in studying sporadic cases of late-onset AD, which display age-related cognitive impairment and many pathological features of AD, including an abnormal expression of anti-aging factors, oxidative stress, inflammation,  $A\beta$  deposits, tau hyperphosphorylation, endoplasmic reticulum stress, abnormal autophagy activity, and disruption of intestinal flora.<sup>43</sup> In addition, the SAMR1 mice with normal senescence phenotypes are commonly used as a background control of the SAMP8 mice. Therefore, the SAMP8 mouse was also an appropriate animal model in researching drugs for sAD.

From the perspective of nutrition, anthocyanins show great preventive and therapeutic potential of AD.<sup>44</sup> Further, as natural compounds, anthocyanins are safer and easier to obtain. We choose a berry anthocyanin, Cy3Gal, which is absorbed faster in the body to intervene in the progress of aging of mice. We found that glucose metabolism in the mice brains declined with aging, while the glucose metabolism in different regions of the brain did not show a significant decrease after Cy3Gal administration. Among different regions of the brain, the olfactory bulb was the cause of concern. The glucose metabolism in the olfactory bulb, where  $A\beta$  was easily accumulated, decreased significantly with aging. Comparably, Cy3Gal had less effect on the glucose metabolism and accumulation of  $A\beta$  in this region (Supplementary Figures 2 and 7). Previous studies have shown that patients with AD developed olfactory dysfunction before  $A\beta$  deposition and cognitive impairment.<sup>45</sup> The present results suggested that the olfactory bulb region was sensitive to aging, and the region may be used as a target area for detecting glucose metabolic rate, which could be used to predict or diagnose AD in the early stage.

Mitochondria is the site of energy metabolism in eukaryotes, and only when it maintains normal functions, can it provide sufficient fuel to support nerve cell function. When the level of mitochondrial energy metabolism is decreased, it will affect insulin signal transduction, glucose receptor changes, and the metabolic phenotype of astrocytes, thus accelerating the onset of AD.<sup>46</sup> In addition, the neuron apoptosis regulated by mitochondria is also an important reason for the pathogenesis of AD.<sup>47</sup> Apoptosis occurs in the early stage of AD. Neuron loss in the brain is one of the most important pathological features of AD. We found that Cy3Gal attenuated apoptosis in the brain of mice with aging, especially neuronal damage in the hippocampus and cerebral cortex (Figure 2 and Supplementary Figure 5). The apoptosis of neurons in CA1 and DG areas of mice hippocampus might lead to the impairment of nerve cells, obstruction of signal transduction, and decline of cognition in mice as observed in the MWM test (Figure 4). In particular,

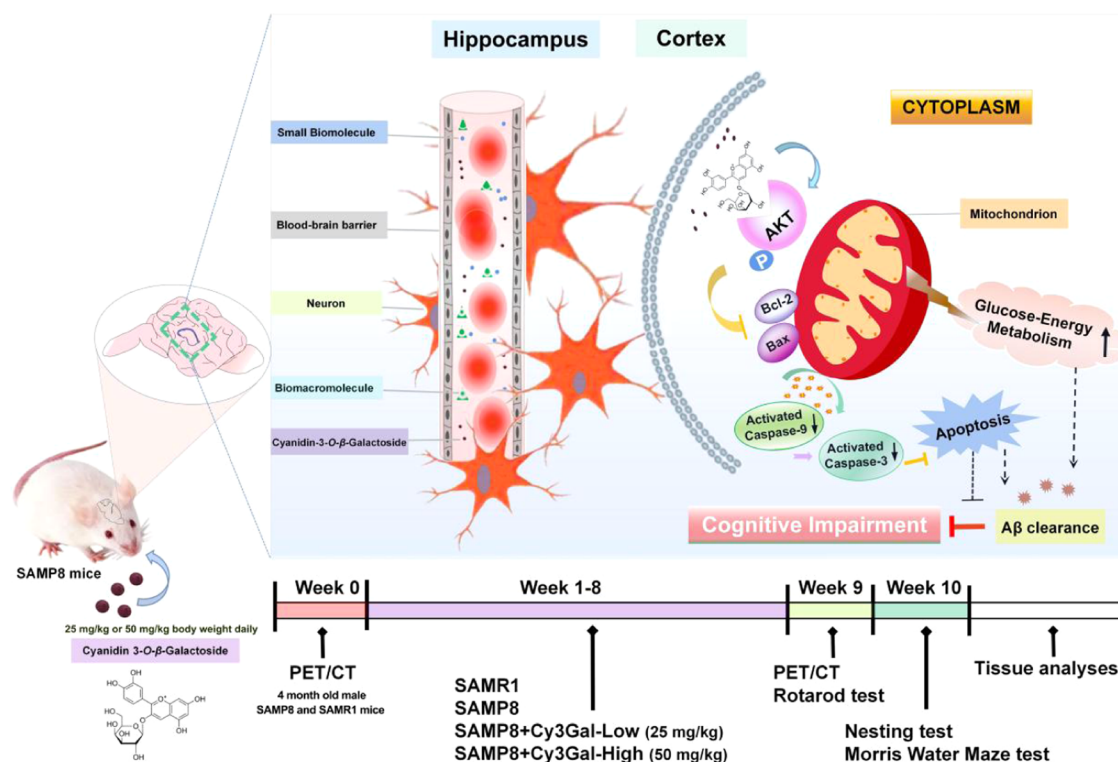


**Figure 7.** Schematic diagram representing the mechanism of Cy3Gal improving cognitive impairment in AD model SAMP8 mice (upper panel) and animal experiment protocols (lower panel).

the Bcl-2 family proteins, the key factors for mitochondrial quality control, are involved in the regulation of mitochondrial autophagy, apoptosis, mitosis, and fusion.<sup>48,49</sup> Cy3Gal increased the Bcl-2 expression in the brain tissue of aged mice, which inhibited the activation of the caspase apoptosis pathway, and effectively protected nerve cells in the cerebral cortex and hippocampus (Figures 2 and 3 and Supplementary Figure 5). In addition, nesting behavior was improved by Cy3Gal in the SAMP8 mice (Supplementary Figure 8), which might be closely related to the improvement of hippocampal function.<sup>26</sup> To find out the molecular targets, and to explain the pathway of Cy3Gal regulating on energy metabolism and mitochondrial function, we majored in the key upstream modulators. PI3K/Akt axis is widely concerned because it is the pathogenic node in almost all major aging diseases. The PI3K/Akt pathway plays an important role in key events in AD, such as metabolic control, stress response, synaptic plasticity, protein stability, and so on.<sup>34</sup> In addition, the PI3K/Akt pathway is an important regulator of the cell energy metabolism that is involved in the intracellular glucose uptake and metabolism. Akt can induce the expression of glycolytic enzymes and promote the expression and recruitment of glucose receptors on the cell membrane.<sup>50</sup> Akt was activated by Cy3Gal in this study (Figure 6A). The molecular docking showed that Cy3Gal was bound in the hydrophobic cavity of Akt with hydrogen bonds and hydrophobic interaction (Figure 6B,C). On the other hand, Cy3Gal has “neural availability”, which promoted it to a target of Akt and caused downstream signal cascade. However, it is hard to conclude that the downstream factors of Akt are only the way to indirectly regulate energy metabolism and neuron apoptosis. This is because there are also some other signal proteins that play an important role in the pathways, just like glycogen synthase

kinase-3 $\beta$  (GSK-3 $\beta$ ), mammalian target of rapamycin (mTOR).<sup>51,52</sup> They are always used as targets for AD drug development and research.<sup>53</sup>

Based on the results of our study, the effects of Cy3Gal on alleviating cognitive impairment caused by aging can be concluded in Figure 7. We demonstrated that an 8-week intervention with Cy3Gal improved the glucose uptake in the mice brains during aging and ameliorated the pathologic changes, such as neuronal damage, A $\beta$  expression, and mitochondrial dysfunction, displaying great effects on spatial learning and memory impairments in aged mice. The results confirmed the efficacy of Cy3Gal in improving cognition and neuroprotection against energy metabolism challenges in mice brains with aging. Akt may be a target for Cy3Gal to exert early benefits against AD. Our study reveals a promising nutritional strategy at the interface of healthy brain aging.

## ■ ASSOCIATED CONTENT

### Supporting Information

The Supporting Information is available free of charge at <https://pubs.acs.org/doi/10.1021/acs.jafc.1c06240>.

Supplementary Figures 1–11 and Supplementary Tables 1 and 2 (PDF)

## ■ AUTHOR INFORMATION

### Corresponding Authors

Jingming Li – College of Food Science and Nutritional Engineering, China Agricultural University, Beijing 100083, China; [orcid.org/0000-0001-9026-8817](https://orcid.org/0000-0001-9026-8817); Email: [lijingming@cau.edu.cn](mailto:lijingming@cau.edu.cn)

Jiachen Zang – College of Food Science and Nutritional Engineering, China Agricultural University, Beijing 100083,

China; [orcid.org/0000-0003-0566-9726](https://orcid.org/0000-0003-0566-9726);

Email: zangjiachen@cau.edu.cn

## Authors

**Zhuoyan Fan** – College of Food Science and Nutritional Engineering, China Agricultural University, Beijing 100083, China

**Haichao Wen** – College of Food Science and Nutritional Engineering, China Agricultural University, Beijing 100083, China

**Xiaoxu Zhang** – College of Food Science and Nutritional Engineering, China Agricultural University, Beijing 100083, China

Complete contact information is available at:

<https://pubs.acs.org/10.1021/acs.jafc.1c06240>

## Notes

The authors declare no competing financial interest.

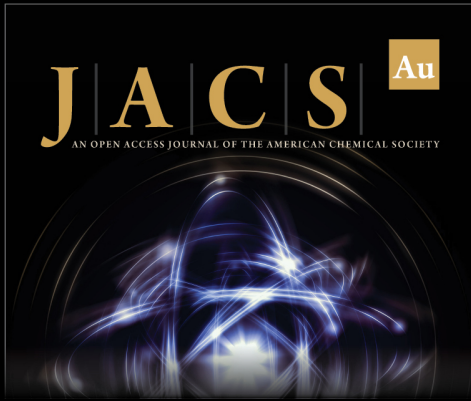
## ACKNOWLEDGMENTS

This work was supported by the National Natural Science Foundation of China (No. 32172210), and Research and development project of functional dietary supplements for special populations (NO: SJ2021002006).

## REFERENCES

- (1) Bachurin, S. O.; Bovina, E. V.; Ustyugov, A. A. Drugs in Clinical Trials for Alzheimer's Disease: The Major Trends. *Med. Res. Rev.* **2017**, *37*, 1186–1225.
- (2) Yiannopoulou, K. G.; Anastasiou, A. I.; Zachariou, V.; Pelidou, S. H. Reasons for Failed Trials of Disease-Modifying Treatments for Alzheimer Disease and Their Contribution in Recent Research. *Biomedicines* **2019**, *7*, No. 97.
- (3) de la Torre, J. C.; Gonzalez-Lima, F. The FDA Approves Aducanumab for Alzheimer's Disease, Raising Important Scientific Questions. *J. Alzheimers Dis.* **2021**, *82*, 881–882.
- (4) Hutton, M.; Mcgowan, E. Clearing Tau Pathology with A $\beta$  Immunotherapy—Reversible and Irreversible Stages Revealed. *Neuron* **2004**, *43*, 293–294.
- (5) Dos Santos Picanco, L. C.; Ozela, P. F.; de Fatima, D. B. B. M.; Pinheiro, A. A.; Padilha, E. C.; Braga, F. S.; de Paula, D. S. C.; Dos, S. C.; Rosa, J.; Da, S. H. L. Alzheimer's Disease: A Review from the Pathophysiology to Diagnosis, New Perspectives for Pharmacological Treatment. *Curr. Med. Chem.* **2018**, *25*, 3141–3159.
- (6) Alzheimer's Disease International. World Alzheimer Report, 2015.
- (7) Tavallaie, M.; Voshtani, R.; Deng, X.; Qiao, Y.; Jiang, F.; Collman, J. P.; Fu, L. Moderation of mitochondrial respiration mitigates metabolic syndrome of aging. *Proc. Natl. Acad. Sci. U.S.A.* **2020**, *117*, 9840–9850.
- (8) Rossi, S.; et al. Brain temperature, body core temperature, and intracranial pressure in acute cerebral damage. *J. Neurol. Neurosurg. Psychiatry* **2001**, *71*, 448–454.
- (9) Cisternas, P.; Inestrosa, N. C. Brain glucose metabolism: Role of Wnt signaling in the metabolic impairment in Alzheimer's disease. *Neurosci. Biobehav. Rev.* **2017**, *80*, 316–328.
- (10) Cunnane, S. C.; Trushina, E.; Morland, C.; Prigione, A.; Casadesus, G.; Andrews, Z. B.; Beal, M. F.; Bergersen, L. H.; Brinton, R. D.; Monte, S.; et al. Brain energy rescue: an emerging therapeutic concept for neurodegenerative disorders of ageing. *Nat. Rev. Drug Discovery* **2020**, *19*, 609–633.
- (11) Folch, J.; Olloquequi, J.; Ettcheto, M.; Busquets, O.; Sánchez-López, E.; Cano, A.; Espinosa-Jiménez, T.; García, M. L.; Beas-Zarate, C.; Casadesús, G.; et al. The Involvement of Peripheral and Brain Insulin Resistance in Late Onset Alzheimer's Dementia. *Front. Aging Neurosci.* **2019**, *11*, No. 236.
- (12) Camandola, S.; Mattson, M. P. Brain metabolism in health, aging, and neurodegeneration. *EMBO J.* **2017**, *36*, 1474–1492.
- (13) Nasrallah, I.; Dubroff, J. An Overview of PET Neuroimaging. *Semin. Nucl. Med.* **2013**, *43*, 449–461.
- (14) Xiong, R.; Wang, X. L.; Wu, J. M.; Tang, Y.; Wu, A. G.; et al. Polyphenols isolated from lychee seed inhibit Alzheimer's disease-associated Tau through improving insulin resistance via the IRS-1/PI3K/Akt/GSK-3 $\beta$  pathway. *J. Ethnopharmacol.* **2020**, *251*, No. 112548.
- (15) Szwajgier, D.; Baranowska-Wójcik, E.; Borowiec, K. Phenolic Acids Exert Anticholinesterase and Cognition-Improving Effects. *Curr. Alzheimer Res.* **2018**, *15*, 531–543.
- (16) Freysson, A.; Page, G.; Fauconneau, B.; Bilan, A. R. Natural stilbenes effects in animal models of Alzheimer's disease. *Neural Regen. Res.* **2020**, *15*, 843–849.
- (17) Li, P.; Feng, D.; Yang, D.; Li, X.; Bai, W.; et al. Protective effects of anthocyanins on neurodegenerative diseases. *Trends Food Sci. Technol.* **2021**, *05*, No. 005.
- (18) Kalt, W.; Blumberg, J. B.; Mcdonald, J. E.; Vinqvist-Tymchuk, M. R.; Fillmore, S.; Graf, B. A.; Leary, J. O.; Milbury, P. E. Identification of anthocyanins in the liver, eye, and brain of blueberry-fed pigs. *J. Agric. Food Chem.* **2008**, *56*, 705–712.
- (19) Milbury, P.; et al. Xenobiotic Metabolism and Berry Flavonoid Transport across the Blood-Brain Barrier. *J. Agric. Food Chem.* **2010**, *58*, 3950–3956.
- (20) Bhaswant, M.; Shafie, S. R.; Mathai, M. L.; Mouatt, P.; Brown, L. Anthocyanins in chokeberry and purple maize attenuate diet-induced metabolic syndrome in rats. *Nutrition* **2017**, *41*, 24–31.
- (21) Faria, A.; Pestana, D.; Teixeira, D.; Azevedo, J.; Freitas, V. D.; Mateus, N.; Calhau, C. Flavonoid transport across RBE4 cells: A blood-brain barrier model. *Cell. Mol. Biol. Lett.* **2010**, *15*, 234–241.
- (22) Wen, H.; Cui, H.; Tian, H.; Zhang, X.; Li, J.; et al. Isolation of Neuroprotective Anthocyanins from Black Chokeberry (*Aronia melanocarpa*) against Amyloid- $\beta$ -Induced Cognitive Impairment. *Foods* **2021**, *10*, No. 63.
- (23) Ichiyani, T.; Shida, Y.; Rahman, M. M.; Hatano, Y.; Konishi, T. Bioavailability and tissue distribution of anthocyanins in bilberry (*Vaccinium myrtillus* L.) extract in rats. *J. Agric. Food Chem.* **2006**, *54*, 6578–6587.
- (24) Koivisto, H.; et al. Progressive age-dependent motor impairment in human tau P301S overexpressing mice. *Behav. Brain Res.* **2019**, *376*, No. 112158.
- (25) Ooigawa, H.; Nawashiro, H.; Fukui, S.; Otani, N.; Osumi, A.; Toyooka, T.; Shima, K. The fate of Nissl-stained dark neurons following traumatic brain injury in rats: difference between neocortex and hippocampus regarding survival rate. *Acta Neuropathol.* **2006**, *112*, 471–481.
- (26) Deacon, R. M. Assessing nest building in mice. *Nat. Protoc.* **2006**, *1*, 1117–1119.
- (27) Magistretti, P. J.; Allaman, I. Lactate in the brain: from metabolic end-product to signalling molecule. *Nat. Rev. Neurosci.* **2018**, *19*, 235–249.
- (28) Beyer, T.; Townsend, D. W.; Brun, T.; Kinahan, P. E.; Charron, M.; Roddy, R.; Jerin, J.; Young, J.; Byars, L.; Nutt, R. A combined PET/CT scanner for clinical oncology. *J. Nucl. Med.* **2000**, *41*, 1369.
- (29) Dos Santos Picanco, L. C.; Ozela, P. F.; Maiara, D.; Pinheiro, A. A.; Padilha, E. C.; Braga, F. S.; de Paula Da Silva, C. H. T.; Santos, C. D.; Rosa, J.; Hage-Melim, L. S. Alzheimer's Disease: A Review from the Pathophysiology to Diagnosis, New Perspectives for Pharmacological Treatment. *Curr. Med. Chem.* **2016**, *23*, 3141–3159.
- (30) Fiandalo, M. V.; Kyprianou, N. Caspase control: protagonists of cancer cell apoptosis. *Exp. Oncol.* **2012**, *34*, 165–175.
- (31) Wu, R.; Tang, S.; Wang, M.; Xu, X.; Chen, Y.; Wang, S. MicroRNA-497 Induces Apoptosis and Suppresses Proliferation via the Bcl-2/Bax-Caspase9-Caspase3 Pathway and Cyclin D2 Protein in HUVECs. *PLoS One* **2016**, *11*, No. e0167052.
- (32) Wesson, D. W.; Donald, A. W. Age and gene overexpression interact to abolish nesting behavior in Tg2576 amyloid precursor protein (APP) mice. *Behav. Brain Res.* **2011**, *216*, 408–413.

- (33) Herholz, K.; Ebmeier, K. Clinical amyloid imaging in Alzheimer's disease. *Lancet Neurol.* **2011**, *10*, 667–670.
- (34) O'Neill, C. PI3-kinase/Akt/mTOR signaling: Impaired on/off switches in aging, cognitive decline and Alzheimer's disease. *Exp. Gerontol.* **2013**, *48*, 647–653.
- (35) Weiner, M. W.; Veitch, D. P.; Aisen, P. S.; Beckett, L. A.; Trojanowski, J. Q. 2014 Update of the Alzheimer's Disease Neuroimaging Initiative: A review of papers published since its inception. *J. Alzheimers Dis.* **2015**, *11*, No. e1-120.
- (36) Chen, Z.; Zhong, C. Decoding Alzheimer's disease from perturbed cerebral glucose metabolism: Implications for diagnostic and therapeutic strategies. *Prog. Neurobiol.* **2013**, *108*, 21–43.
- (37) Willette, A. A.; Bendlin, B. B.; Starks, E. J. Association of Insulin Resistance With Cerebral Glucose Uptake in Late Middle-Aged Adults at Risk for Alzheimer Disease (vol 72, pg 1013, 2015). *JAMA Neurol.* **2017**, *72*, 1013–1020.
- (38) Chou, J. L.; Shenoy, D. V.; Thomas, N.; Choudhary, P. K.; Laferla, F. M.; Goodman, S. R.; Breen, G. Early dysregulation of the mitochondrial proteome in a mouse model of Alzheimer's disease. *J. Proteomics* **2011**, *74*, 466–479.
- (39) Mosconi, L.; Andrews, R. D.; Matthews, D. C. Comparing brain amyloid deposition, glucose metabolism, and atrophy in mild cognitive impairment with and without a family history of dementia. *J. Alzheimers Dis.* **2013**, *35*, 509–524.
- (40) Szutowicz, A.; Bielarczyk, H.; Ronowska, A.; Gul-Hinc, S.; Klimaszewska-Ata, J.; Dy, A.; Zy, K.M.; Pawe Czyk, T. Intracellular redistribution of acetyl-CoA, the pivotal point in differential susceptibility of cholinergic neurons and glial cells to neurodegenerative signals. *Biochem. Soc. Trans.* **2014**, *42*, 1101.
- (41) Ribeiro, M. F.; Genebra, T.; Rego, A. C.; Rodrigues, C.; Solá, S. Amyloid  $\beta$  Peptide Compromises Neural Stem Cell Fate by Irreversibly Disturbing Mitochondrial Oxidative State and Blocking Mitochondrial Biogenesis and Dynamics. *Mol. Neurobiol.* **2019**, *56*, 3922–3936.
- (42) Zetterberg, H.; Mattsson, N. Understanding the cause of sporadic Alzheimer's disease. *Expert Rev. Neurother.* **2014**, *14*, 621–630.
- (43) Liu, B.; Liu, J.; Shi, J. S. SAMP8 Mice as a Model of Age-Related Cognition Decline with Underlying Mechanisms in Alzheimer's Disease. *J. Alzheimers Dis.* **2020**, *75*, 385–395.
- (44) Lakey-Beitia, J.; Berrocal, R.; Rao, K. S.; Durant, A. A. Polyphenols as Therapeutic Molecules in Alzheimer's Disease Through Modulating Amyloid Pathways. *Mol. Neurobiol.* **2015**, *51*, 466–479.
- (45) Chen, M.; Chen, Y.; Huo, Q.; Wang, L.; Yang, L.; et al. Enhancing GABAergic signaling ameliorates aberrant gamma oscillations of olfactory bulb in AD mouse models. *Mol. Neurodegener.* **2021**, *16*, No. 14.
- (46) Yin, F.; Sancheti, H.; Liu, Z.; Cadenas, E. Mitochondrial function in ageing: coordination with signalling and transcriptional pathways. *J. Physiol.* **2016**, *594*, 2025–2042.
- (47) Ghavami, S.; Shahla, S.; Behzad, Y.; Sudharsana, R. A.; Jaganmohan, R. J.; Maryam, M.; Jonas, C.; Wiem, C.; Adel, R. M.; Hessam, H. K.; et al. Autophagy and apoptosis dysfunction in neurodegenerative disorders. *Prog. Neurobiol.* **2014**, *112*, 24–49.
- (48) Karbowski, M.; Norris, K. L.; Cleland, M. M.; Jeong, S. Y.; Youle, R. J. Role of Bax and Bak in mitochondrial morphogenesis. *Nature* **2006**, *443*, 658–662.
- (49) Hollville, E.; Carroll, R.; Cullen, S.; Martin, S. Bcl-2 family proteins participate in mitochondrial quality control by regulating Parkin/PINK1-dependent mitophagy. *Mol. Cell* **2014**, *55*, 451–466.
- (50) Bonelli, M.; Terenziani, R.; Zoppi, S.; Fumarola, C.; Monica, S. L.; Cretella, D.; Alfieri, R.; Cavazzoni, A.; Digiaco, G.; Galetti, M.; et al. Dual Inhibition of CDK4/6 and PI3K/AKT/mTOR Signaling Impairs Energy Metabolism in MPM Cancer Cells. *Int. J. Mol. Sci.* **2020**, *21*, No. 5165.
- (51) Zhai, H.; Kang, Z.; Zhang, H.; Ma, J.; Chen, G. Baicalin attenuated substantia nigra neuronal apoptosis in Parkinson's disease rats via the mTOR/AKT/GSK-3 $\beta$  pathway. *J. Integr. Neurosci.* **2019**, *18*, 423–429.
- (52) Zoia, C. P.; Compagnoni, P.; Bazzini, C.; Ferrarese, C.; et al. Alzheimer's Disease & Parkinsonism Can Signaling Molecules in Fibroblasts Detect Prodromal Alzheimer's Disease? *J. Alzheimers Dis. Parkinsonism* **2020**, *10*, No. 1000490.
- (53) Dos Santos Picanco, L. C.; Ozela, P. F.; de Fatima, D. B. B. M.; Pinheiro, A. A.; Padilha, E. C.; Braga, F. S.; de Paula, D. S. C.; Dos, S. C.; Rosa, J.; Da, S. H. L. Alzheimer's Disease: A Review from the Pathophysiology to Diagnosis, New Perspectives for Pharmacological Treatment. *Curr. Med. Chem.* **2018**, *25*, 3141–3159.



**JACS** Au  
AN OPEN ACCESS JOURNAL OF THE AMERICAN CHEMICAL SOCIETY

Editor-in-Chief  
**Prof. Christopher W. Jones**  
Georgia Institute of Technology, USA

**Open for Submissions** 

pubs.acs.org/jacsau  ACS Publications  
Most Trusted. Most Cited. Most Read.